AQUA
Water Infrastructure, Ecosystems and Society

IWA PUBLISHING

 AQUA — Water Infrastructure, Ecosystems and Society Vol 73 No 3, 674 doi: 10.2166/aqua.2024.034

Analysis of upper and lower nappe profiles of large orifice for the design of bottom and roof profiles of high head orifice spillway

Shafqat Hussain Bhatti[a], Habib Ur Rehman[b], Muhammad Kaleem Sarwar[a], Muhammad Waqas Zaffar[c], Muhammad Awais Zafar[a,*] and Muhammad Atiq Ur Rehman Tariq[a]

[a] Centre of Excellence in Water Resources Engineering, University of Engineering and Technology Lahore, Lahore 54890, Pakistan
[b] Department of Civil Engineering, University of Engineering and Technology Lahore, Lahore, Pakistan
[c] Department of Civil Engineering Technology, University of Chenab Gujrat, Gujrat, Pakistan
*Corresponding author. E-mail: a.zafar@uet.edu.pk

MAZ, 0009-0004-3534-0125

ABSTRACT

Large orifices are constructed for dams to release water and sediments from reservoirs. Such structures are called submerged spillways. Numerous studies have investigated discharge coefficient, velocity coefficient, and head loss coefficient of large orifices; however, the literature lacks data on the upper and lower nappes of the jets from these orifices. In the present experimental study, the upper and lower nappes are investigated up to 80 m head at different gate openings. The observed minor deviation between the lower nappe profile and trajectory profile equation suggests sensitivity to different factors. The significant role of the coefficient of velocity, averaging at 0.926, highlights its impact on minor deviation. Subsequently, the impact of the solid bottom profile on the discharge coefficient and upper nappe profile are also examined. The results show improvement in discharge coefficient of a sharp-edged large orifice, which increased from 0.69 to 0.74. The results also indicate that the upper nappe profiles and United States Bureau of Reclamation (USBR) profiles are similar. The improvement in the upper nappe profile indicates the significant role of the solid bottom profile, which consequently was found to be helpful in defining the roof profile of an orifice spillway. .

Key words: large orifice, lower profile, orifice spillway, physical modelling, upper profile

HIGHLIGHTS

- Hydraulic analyses of lower and upper nappe profiles of sharp-edged large orifices.
- Impact evaluation of a solid bottom profile on an upper nappe profile.
- Hydraulic performance evaluation of solid bottom profile at various operational scenarios.

GRAPHICAL ABSTRACT

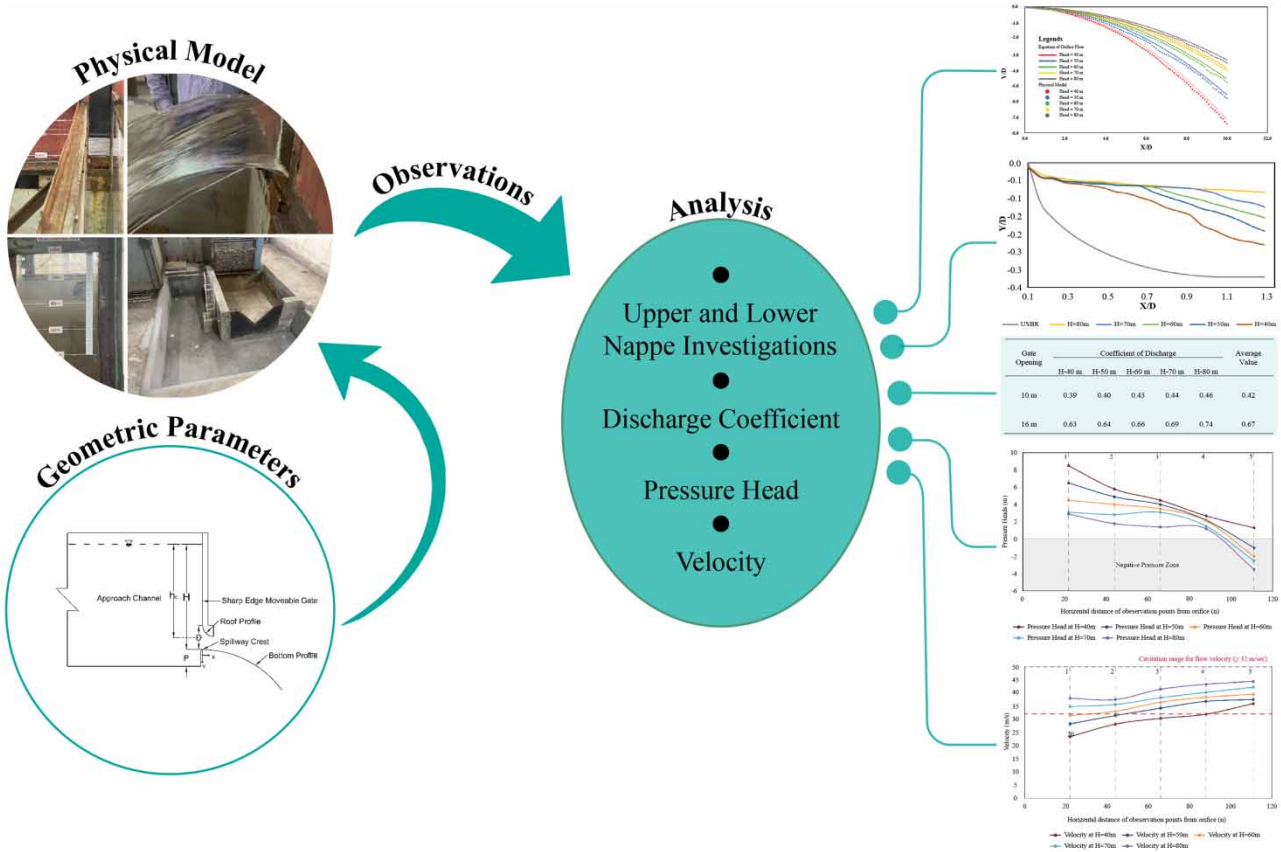

NOTATIONS

D	gate opening/height of orifice
b	width of orifice
Re	Reynolds number
Fr	Froude number
We	Weber number
H	operating head
C_d	discharge coefficient
Qth	theoretical discharge
h	water level in stilling well of V-notch.
h_c	center line head over the orifice
C_v	coefficient of velocity
x, y	horizontal and vertical coordinates of lower nappe profile
x_1, y_1	horizontal and vertical coordinates of upper nappe profile

1. INTRODUCTION

An orifice is an opening constructed in a dam structure to regulate the flow. The large rectangular orifices are generally constructed to pass the surplus flows and are used to dispose of the river sediments. Velocities more than 25 m/s over the spillway crest and discharge intensities of 200–300 m^3/s/m make the design of the orifice spillway both complex and involved, requiring detailed investigation during planning besides studies on a scaled model (Bhosekar *et al.* 2014). However, the operation of these spillways also creates complicated issues, such as turbulence, sediment transport (Pu *et al.* 2014, 2016), natural bed forms (Pu *et al.* 2017), and cavitation (Sarwar *et al.* 2016). During spillway operation, energy dissipation of

flowing water depends upon the Froude Number (Fr. No.). The higher the Fr. No., the greater the dissipation of energy. In vertical shafts, flow energy dissipation efficiency (η_s) decreases with increasing Fr. No. It was found to be between 10.80 and 62.29% (Mohmoudi-Rad & Najafzadehhe 2022, 2023). The size of an orifice is influenced by several factors such as water head, which is classified into three different categories i.e., Low Head, Medium Head, and High Head Orifice. A need for a physical and numerical model for modelling orifice spillway flows was identified. The discharge coefficient (C_d) was found in the range of 0.831–0.942 (Bos 1989; Swamee *et al.* 1998; Gadge *et al.* 2019; Mozaffari *et al.* 2022). Additionally, the actual size of the orifice may vary depending on the specific design requirements of the dam while other parameters that affect the size of the orifice are flow rates, size of reservoir, and expected floods (Amirkhani *et al.* 2017; Bhattarai & Sharma 2017).

Numerous studies investigated hydraulic coefficients for the flow through an orifice, but coefficient of discharge, coefficient of velocity, and head loss coefficient (Essien *et al.* 2019; Hussain *et al.* 2014) are the most significant ones and play vital roles to control, measure, and regulate the flow in the design and operation of orifices. Essien *et al.* 2019 conducted an experimental investigation on C_d. An empirical correlation between discharge coefficient and size of orifice was developed. C_d values obtained from experimental data and those from the empirical correlation were compared, and a mean standard deviation of 0.0231 was obtained. In addition, these parameters are also used for prediction of flow and energy loss (Babu *et al.* 2018; Manzano-Miura *et al.* 2022). Roof and bottom profiles of orifice spillways are important parts of orifice spillway geometry. These profiles are designed to optimize water discharge and control during spillway operation. The roof profile of an orifice spillway refers to the shape or contour of the structure's top surface, which directs water flow. Meanwhile, the bottom profile refers to the shape or contour of the spillway's lower surface, influencing how water exits the spillway. The design of roof profile and bottom profile has not been standardized (Khatsuria 2013). Vatankhah & Rafeifar (2020) conducted a series of laboratory runs (588 runs) for different values of orifice geometry. Using measurements obtained by laboratory runs, the proposed theoretical models of elliptical side orifices were calibrated under free outflow conditions. The model that includes the approach Froude number had an average error of 1.74%, while the other model that does not include the approach Froude number had an average error of about 2.43%. Haghbin & Sharafati (2022) provided a comprehensive review of the application of soft computing (SC) models for estimating C_d of different flow control structures such as ogee spillways, orifices, and side weirs. Besides, the ratio of orifice crest height to height of side orifice, the ratio of main channel width to length of side orifice, the ratio of main channel width to height of side orifice, and the ratio of the height of the side orifice to upstream flow depth were extensively employed to calculate C_d of orifice structures. Maher *et al.* (2019) investigated the effect of different inlet configurations on the discharge coefficient of large orifices and found that the discharge coefficient was highest for the circular inlet configuration. A study conducted by Bhattarai & Sharma (2017) noted a significant impact of orifice size on the spillway discharge capacity of the embankment dam. Conversely, Jothiprakash *et al.* (2015) noted that the velocity coefficient was affected by the upstream flow condition and the shape of the orifice. Similarly, Jithish & Ajay Kumar (2015) used Computational Fluid Dynamic (CFD) simulations to find out the effect of orifice size, its inlet and outlet configuration, and Reynolds number on the velocity coefficient. Hussain *et al.* (2016) developed relationships for coefficient of discharge for orifices under free and submerged flow conditions through analytical and experimental considerations. The computed discharges using developed relationships were within $\pm 5\%$ and $\pm 10\%$ of the observed ones for free and submerged orifices, respectively. A sensitivity analysis revealed that the discharge through the side orifice is more sensitive to the low head above the centre of the orifice. Apart from free flow and submerged flow conditions for orifice structure, Adam *et al.* (2016), Mali *et al.* (2020), Adam *et al.* (2019), and Wang *et al.* (2020) studied head loss coefficient for the large orifices. These studies focused on orifice size, submergence ratio, and inlet velocity on the head loss coefficient.

From the bibliographic analysis, due to the significance of spillways to discharge the floods safely, in addition to the discharge coefficient, velocity coefficient, and head loss, the study of spillway profiles, i.e., roof and bottom profiles are crucial in the design and operation of spillways. However, except for Gadge *et al.* (2019) who developed design guidelines and equations for the bottom and roof profiles (applicable to orifice spillways with head varying from 30 to 70 m), the literature lacks information on the design of roof profile and bottom profile for 40–80 m heads and 10–16 m orifice openings. Therefore, in the present study, a physical model is developed and operated under different water heads (40–80 m) and gate openings (10–16 m). This research study is focused on orifice spillways by investigating the flows through a sharp-edged large orifice. Understanding of lower and upper nappe profiles of the jet of large orifices may be helpful in determining the bottom and roof profiles of an orifice spillway.

2. MATERIAL AND METHODS

The present study has developed a physical model of 1:100 scale to investigate the roof and bottom profiles of a large orifice spillway. Before developing the physical model, dimensional analysis is carried out to identify the critical hydraulic parameters that affect the roof and bottom profiles of the studied spillway. The details of dimensionless numbers, physical model, and measurement techniques are explained in the proceeding sections 2.1, 2.2, and 2.3, respectively.

2.1. Scale modelling of flows through large orifice

To develop the physical model for a sharp-edged large orifice, dimensional analysis is performed to determine the essential parameters that affect the flow rate through the orifice. Dimensional analysis is a powerful and widely used method that provides insights into the relationships between different physical quantities, aiding in problem-solving and model development in various scientific and engineering domains. In dimensional analysis, physical quantities are classified into different dimensions such as length, mass, and time. The Buckingham Pi theorem, a key tool in dimensional analysis, states that if a physical problem involves 'n' variables and has 'm' fundamental dimensions, it can be expressed in terms of dimensionless quantities. This reduces the complexity of problems and helps in constructing dimensionless groups. In the sharp-edged large orifice, the flow can be affected by various parameters such as width (b) and height (D) of the orifice, horizontal (x) and vertical (y) coordinates of the lower nappe profile, horizontal (x_1) and vertical (y_1) coordinates of the upper nappe profile, fluid density (ρ) and viscosity (μ), surface tension (σ), gravitational acceleration (g), and head above the crest (h_d) (Gadge *et al.* 2016). After employing these parameters, a set of dimensionless parameters are obtained using the Buckingham Pi theorem as follows (Chanson 1999):

$$f\left(\frac{\rho v D}{\mu}, \frac{v}{\sqrt{gD}}, \frac{\rho v^2 D}{\sigma}, \frac{h_d\, b}{D}, \frac{x}{D}, \frac{y}{D}, \frac{x_1}{D}, \frac{y_1}{D}\right) = 0 \tag{1}$$

The dimensionless parameters in Equation (1) are transformed into dimensionless numbers as presented in Equation (2):

$$f\left(\mathrm{Re}, Fr, We, h, AR, \frac{x}{D}, \frac{y}{D}, \frac{x_1}{D}, \frac{y_1}{D}\right) = 0 \tag{2}$$

where *Re*, *Fr*, *We*, h, AR, x/D, y/D, x_1/D, and y_1/D are the Reynolds number, Froude number, Weber number, Head ratio, Orifice aspect ratio, Horizontal lower nappe profile position, Vertical lower nappe profile position, Horizontal upper nappe profile position, and Vertical upper nappe profile position, respectively.

The viscous and surface tension forces have a negligible effect on free surface flows whereas gravitational force has a considerable impact on free surface flows (Rezazadeh *et al.* 2020, Mahtabi & Arvanaghi 2018, and Daneshfaraz *et al.* 2023). Therefore, at present, Froude number similarities are employed to develop the physical model, whereas to minimize the viscous and surface tension forces, Reynolds number ($\mathrm{Re} > 105$) and flow depth over the crest against the design head are employed for deciding the scale of the physical model (USBR 1980; Pfister & Chanson 2014; Pfister & Hager 2014; Gadge *et al.* 2016).

2.2. Development of physical model

The present physical model was developed in the hydraulic laboratory of the Centre of Excellence in Water Resources Engineering (CEWRE), Lahore, Pakistan. A scaled model of 1:100 ratio was constructed and placed in a 1-m wide and 15-m long flume.

After determining the model's scale, a sharp-edged large orifice 10-m wide (Prototype dimension) and 16-m (Prototype dimension) high was placed in the flume. A moveable gate plate was employed to adjust the height of the orifice. Two Perspex sheets were positioned in front of the orifice to mark the profiles of the upper nappe and lower nappe. The flow through the orifice was measured using a V-notch installed in the downstream channel as shown in Figure 1. The model was operated at different heads (H) and gate openings (D). For each of the investigated gate openings, the head was changed from 40 m to 80 m with an increment of 10 m. The value of the Reynolds Number for the present model reached was 9×10^5, which was found to be more than the recommended value ($\mathrm{Re} > 105$) (USBR 1980; Pfister & Chanson 2014; Pfister & Hager 2014; Gadge *et al.* 2016) and the indicated minimum effect for viscous and surface tension forces.

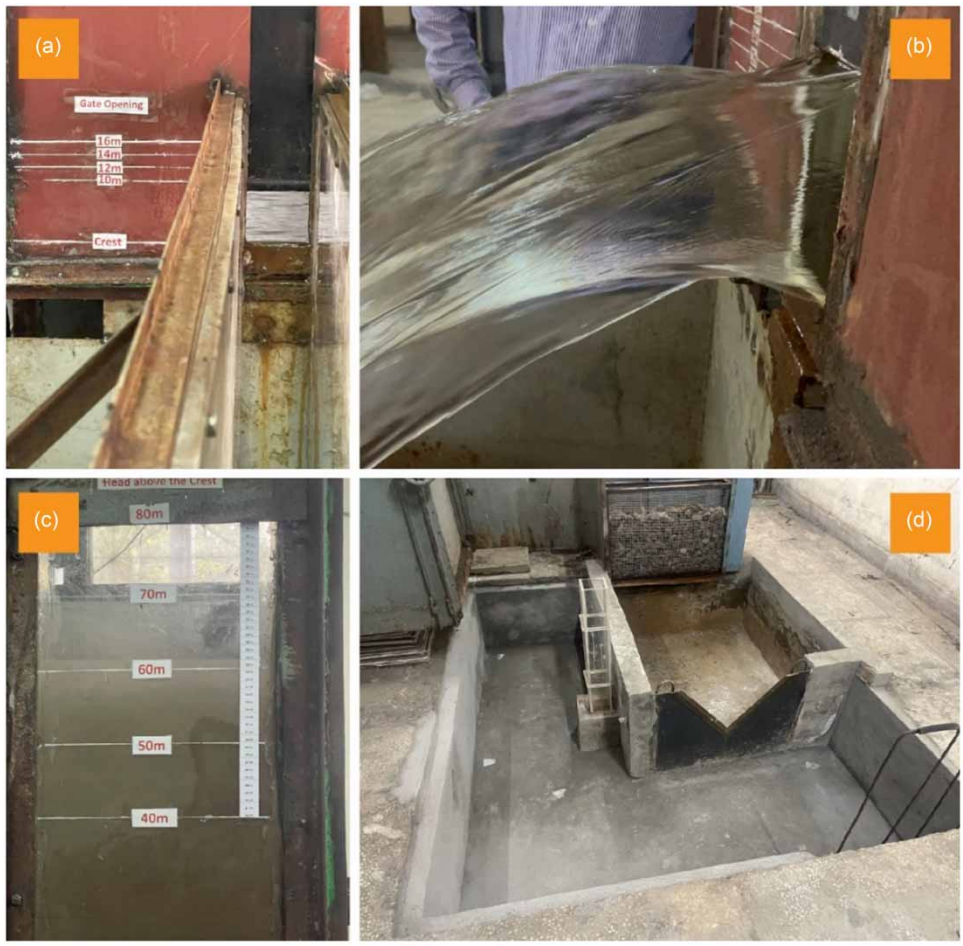

Figure 1 | Physical model of sharp-crested orifice spillway in CEWRE laboratory: (a) front side of the model showing gate opening, (b) side view showing flow through orifice, (c) scale to maintain the head level, (d) flow measurement arrangement downstream of model.

2.3. Lower and upper nappe profile measurements

To maintain the specific reservoir heads, water levels of 40, 50, 60, 70, and 80 m were set in the flume. Free flow discharges were allowed towards the downstream channel of the model and perspex transparent sheets of 1.83 m length were fixed downstream of the orifice (Figure 2) to measure the X and Y coordinates of the lower and upper nappe profiles for the investigated scenarios. The jet profiles through the orifice were sketched on either side of the transparent sheet as shown in Figure 2. The vena contracta occurred when water flowed through an orifice that was found to be contracted on the downstream side because of the high velocities with smaller cross-sectional areas (Prajakta *et al.* 2016). Subsequently, for each scenario, lower and upper nappe profiles were drawn at an interval of 0.01 m (1 cm on model) and were plotted using the non-dimensional parameters i.e., $x/D, y/D, x_1/D$, and y_1/D, where x, y, x_1, and y_1 are the horizontal and vertical distances of upper and lower nappe, respectively, which were measured from the orifice crest, while D is the gate opening as shown in Figure 2.

2.4. Discharge measurement

In the present study, the C_d was computed by the actual flow's measurement. For each experiment, V-notch weir was used to measure the orifice discharge and subsequently the discharge coefficient was computed. A stilling well was installed downstream of the flume. The theoretical discharge through V-notch was computed using the relationship given in Equation (3).

$$Q_{th} = 2.36 \times h^{5/2} \tag{3}$$

where h is the water level at the V-notch in the stilling well.

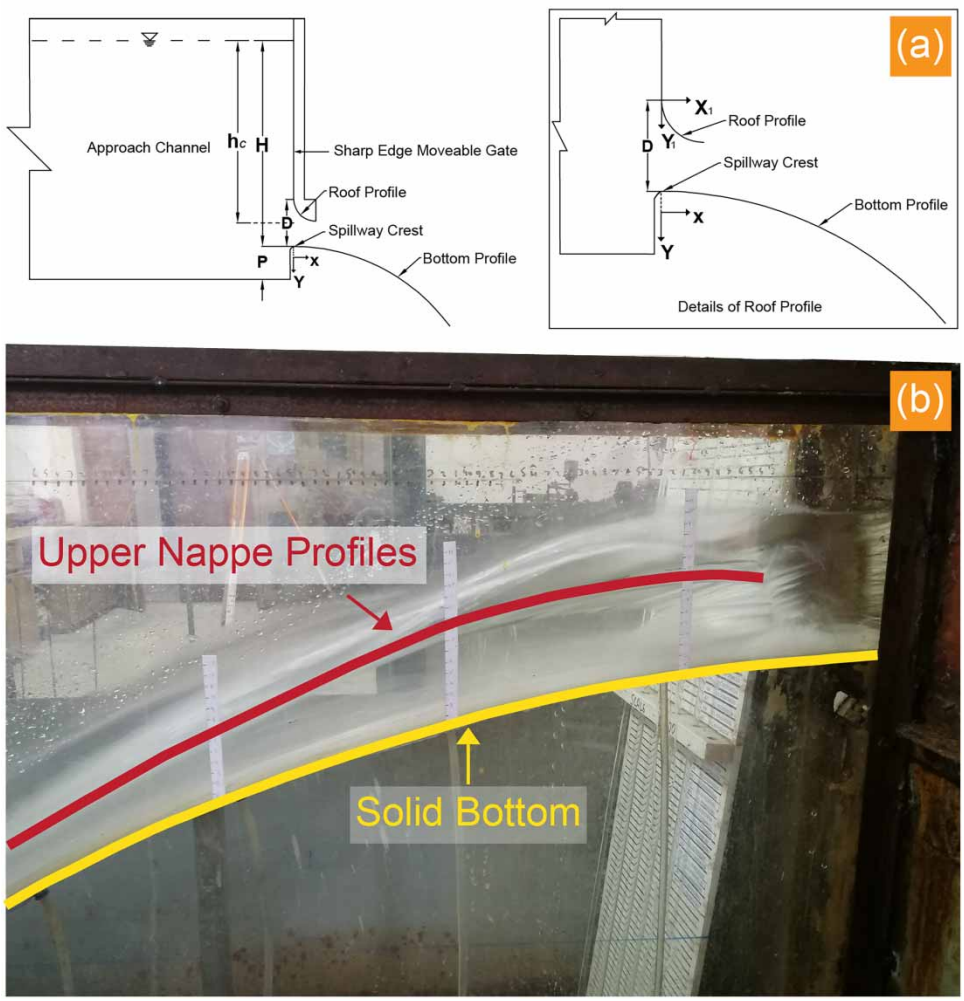

Figure 2 | (a) Details of geometric parameters and (b) the upper nappe profile of a water jet in the model of a large orifice after installing the solid bottom.

3. RESULT AND DISCUSSION

3.1. Coefficient of discharge for sharp-edged orifice

From Table 1 the C_d for a sharp-edged large orifice was found to range between 0.30 and 0.66, which agree with the values of Bansal 2010 and Prajakta *et al.* 2016. The variation in C_d values is the result of different factors such as head range, the size of the orifice, approach velocity, and orifice design and edge sharpness. In Table 1, H is the head above the crest of the orifice.

3.2. Nappe profiles of orifice flows

To develop the solid bottom and roof profiles for orifice spillways (Figure 2), upper and lower nappe profiles are drawn. These profiles are then compared with profiles obtained through the empirical relations 6 and 7.

3.2.1. Lower nappe profiles for sharp-edged large orifice

Figures 3 and 4 compare the lower nappe profiles of the present physical model with the empirical equation at gate opening 10 and 16 m, respectively. The experimental results of the present physical model agree well with the trajectory profile equation ($X^2 = 4yh_c$). However, the physical model showed little deviation from the empirical results due to errors in

Table 1 | C_d values against different configurations of head and gate openings

	C_d					
Gate opening	**H-40 m**	**H-50 m**	**H-60 m**	**H-70 m**	**H-80 m**	**Average Value**
10 m	0.30	0.34	0.33	0.32	0.32	0.32
12 m	0.42	0.42	0.38	0.39	0.37	0.40
14 m	0.44	0.42	0.44	0.46	0.43	0.44
16 m	0.54	0.55	0.55	0.63	0.66	0.59

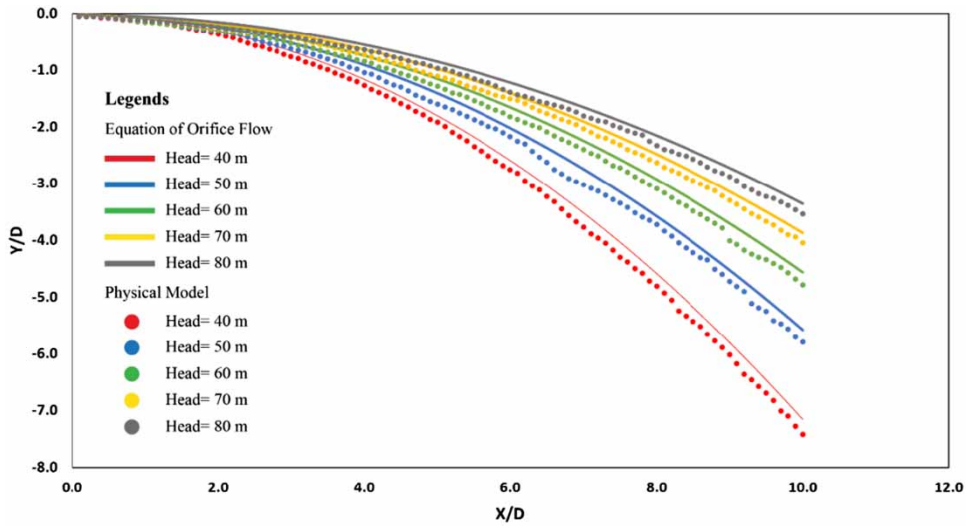

Figure 3 | Comparison of lower nappe profiles at various heads and a 10-m gate opening.

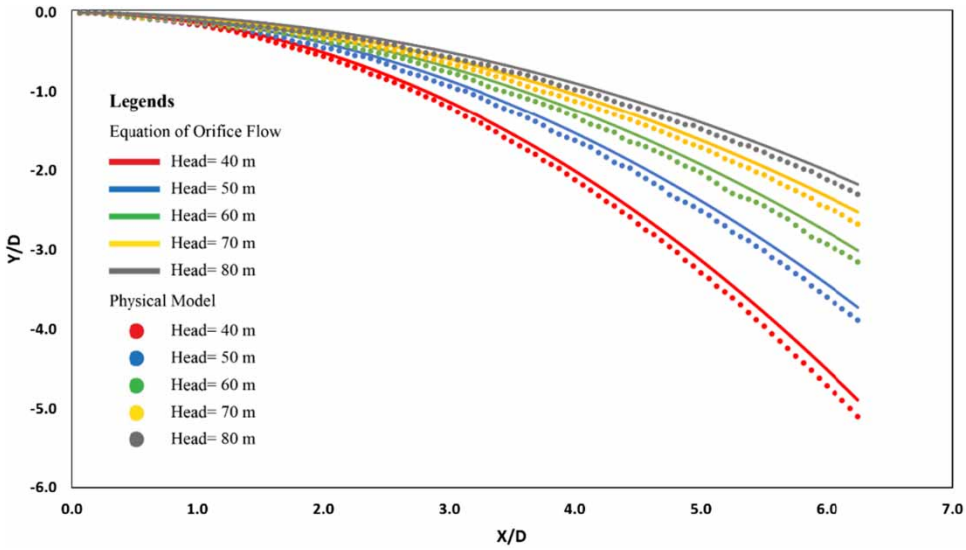

Figure 4 | Comparison of lower nappe profiles at various heads and a 16-m gate opening.

qualitative data and scale affects. The profiles obtained through trajectory equation are affected by the coefficient of velocity.

$$Cv^2 = \frac{X^2}{4yh_c} \tag{4}$$

where in the Equation (4), x and y denote the horizontal and vertical distances of the nappe profiles from the orifice opening, respectively, while h_c is the centre line head over the orifice as shown in Figure 2.

Conversely, for an orifice spillway, the bottom nappe profile is always seen to be parabolic shaped (Figure 2), which can be derived using Equations (5) and (6).

$$X^2 = kyh_c \tag{5}$$

where the coefficient k affects the shape of the parabolic profile. From the bibliographic analysis, it is found that for the flows from the sharp-edged orifices, the coefficient of velocity is approximately equal to unity, which indicates streamline flow through the sharp-edged orifices (Lienhard 1984; Prajakta *et al.* 2016). Therefore, Equation (6) is used to draw comparison for bottom profiles obtained from the present experimental results, which are expressed as:

$$X^2 = 4yh_c \tag{6}$$

From the experiments, the values of the C_v were found to be ranged between 0.894 and 0.947 with an averaged value of 0.926. The variation in the C_v value was due to the change in k values. The results further indicated that any change in the values of C_v and k directly affected the lower profile of the orifice. For different heads and orifice gate openings, values of k and C_v are presented in Table 2.

From the results, it is found that the k value is ranged between 3.27 and 3.630, while the literature has indicated a maximum value of 4. In comparison to the conventional value of 4, the lower value of k significantly affected the curvature of the profile, which further resulted in a steeper curve. After employing the k values, the trends of the bottom profile of the orifice spillway are found to be in good agreement with the empirical data ($X^2 = kyh_c$).

3.2.2. Upper nappe profile for sharp-edged large orifice

Figure 5 compares the non-dimensional plots between the present results of the physical model with the USBR empirical equation. The curves of five different upper nappe profiles are drawn by changing the orifice gate openings (from 10 to 16 m) at different water levels, i.e., 40–80 m After computing the profiles using the USBR Equation (7), the profiles are found to be elliptical in shape as presented in Figure 5.

$$\frac{X^2}{D^2} + \frac{y^2}{(0.32D)^2} = 1 \tag{7}$$

Table 2 | Coefficient of velocity (C_v) and constant (k) in the physical model

Gate Opening (m)	Head (m)	Coefficient of velocity (C_v)	Constant (k)
10	40	0.894	3.278
	50	0.904	3.446
	60	0.912	3.386
	70	0.925	3.468
	80	0.933	3.606
16	40	0.890	3.497
	50	0.909	3.373
	60	0.918	3.407
	70	0.930	3.513
	80	0.947	3.630

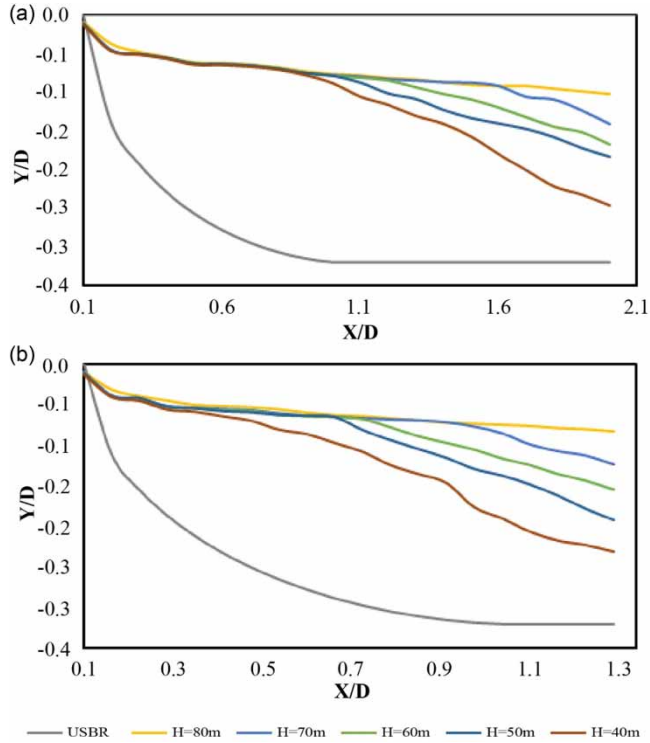

Figure 5 | Comparison of upper nappe profiles with the USBR profile at (a) a 10-m gate opening and (b) a 16-m gate opening.

where x and y are the coordinates of the elliptical profiles and D is the gate opening. Equation (7) indicates that the elliptical profile, being a quarter of an ellipse, lacked a direct correlation with variations in head. Thereby only one profile is plotted using the USBR equation. Hence, profiles obtained from physical model observations are subjected to a comparative analysis with the USBR profile. After comparing with the USBR (1987) upper nappe profile, the results of the present model show deviations as can be seen in Figure 5. The difference in the profiles is found to be high because these profiles are drawn without considering the solid bottom profile of the orifice.

Considering this significant difference in the upper nappe profiles of the present study and the existing literature representing the USBR approach, the observed upper nappe profiles in this study cannot be directly applicable for determining the roof profile of an orifice spillway. Therefore, in the following section, the impact of the solid bottom profile on the upper nappe profile in the form of experimental results is presented.

3.2.3. Significance of solid bottom profile for upper nappe of large orifice

The solid bottom profile of metal was prepared using Equation (6). It was fixed downstream of a sharp-edged large orifice (Figure 2). The model was operated with different water heads and gate openings. Figure 6 illustrates the comparison between the observed upper nappe profiles (with and without a solid bottom) and the USBR profile (1987). The comparison reveals the significant difference in the values of the upper nappe profile with and without the solid bottom profiles. However, the profile with solid bottom shows close agreement with the USBR (1987) profile and further indicates that the solid bottom profile plays a crucial role in determining the accurate upper nappe profiles as shown in Figure 6.

3.2.4. Impact of solid bottom profile on coefficient of discharge

The solid bottom profile as shown in Figure 2 plays a crucial role in influencing the discharge coefficient of the orifice. Table 3 shows an improvement in the discharge coefficient on installation of the solid bottom profile as compared with the results of Table 1. The discharge coefficient varies from 0.39 to 0.74. This range of discharge coefficients is more than that without a solid bottom. The solid bottom profile was developed by analysing lower nappe profiles and using the equation $X^2 = 4yh_c$. It helped in maintaining a consistent pressure distribution, reducing losses, and ultimately improving the discharge coefficient.

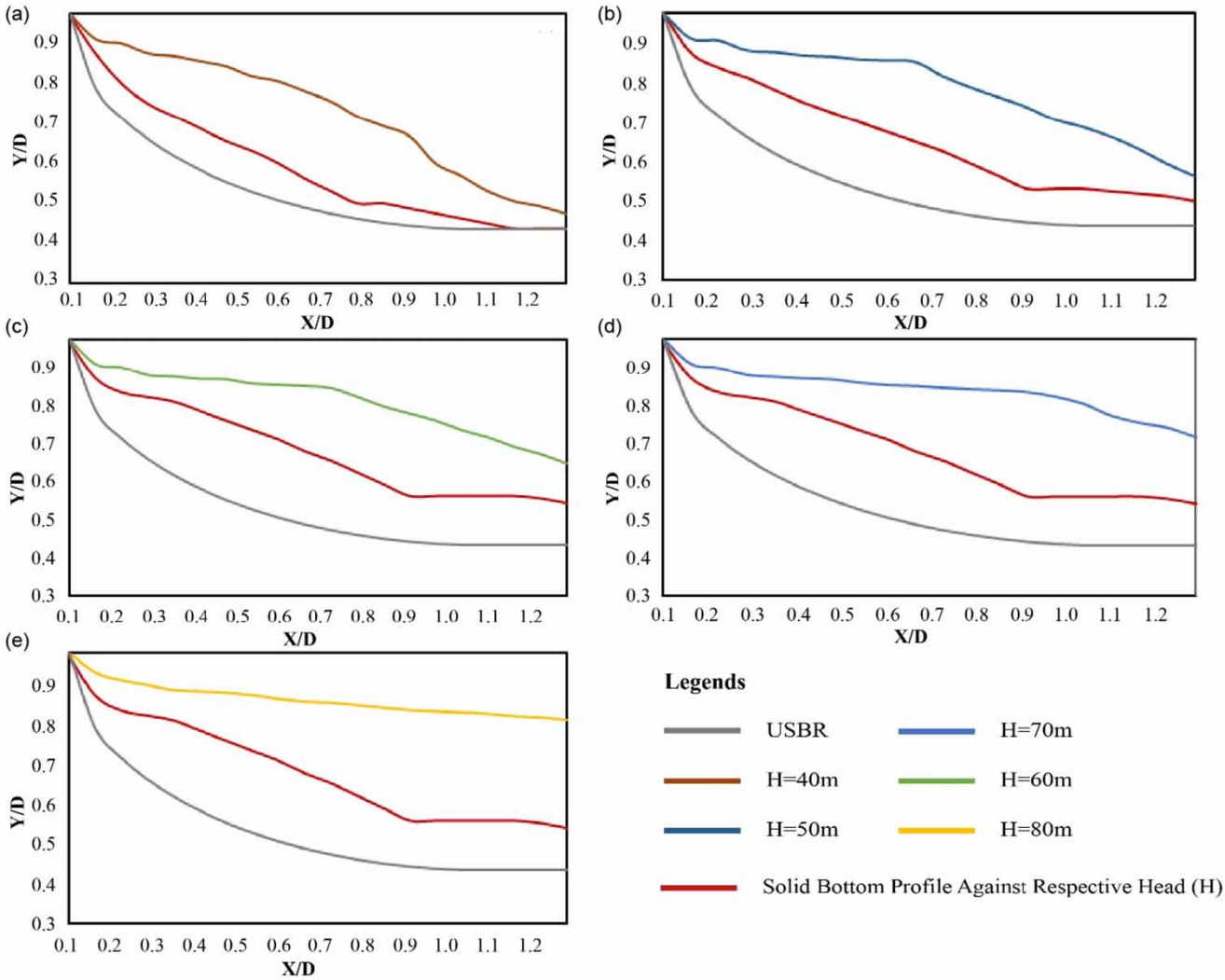

Figure 6 | Comparison of upper nappe profiles (with and without a solid bottom) with USBR at (a) 40-m head, (b) 50 m head, (c) 60-m head, (d) 70-m head, and (e) 80 m head profile against a 16-m gate opening.

Table 3 | Discharge coefficient after installing solid bottom profile

	Coefficient of Discharge					
Gate opening	H-40 m	H-50 m	H-60 m	H-70 m	H-80 m	Average value
10 m	0.39	0.40	0.43	0.44	0.46	0.42
16 m	0.63	0.64	0.66	0.69	0.74	0.67

3.3. Pressure and velocity distribution along a solid bottom profile

Orifice spillways are generally operated at gated condition. Hence, there may be the possibility of occurrence of negative pressures on spillway bottom profiles downstream of the gate for operation of small gate openings (Nguyen & Wang 2015). In view of this context, bottom profiles (Figure 2) proposed in the paper were tested mainly in terms of pressure distribution. For measurement of pressure and velocity, five observation points were marked at different locations along the solid bottom profiles. The results indicated that the pressure distribution along the bottom profile is found to be dynamic, changing

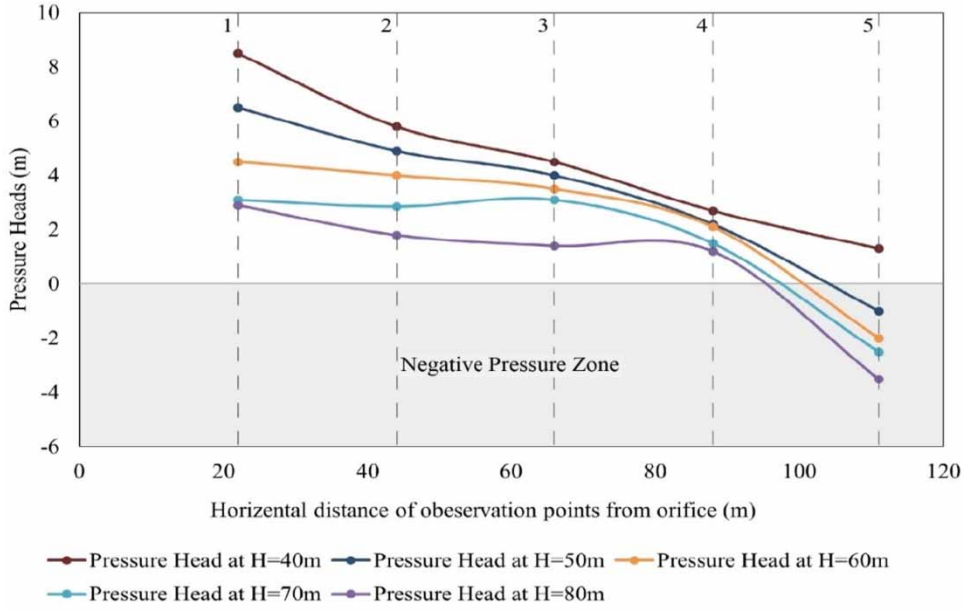

Figure 7 | Pressure head variation along the bottom profile (chute) at various heads and a 16-m gate opening.

as the flow travelled towards the downstream side, as can be seen in Figure 7. At the first observation point, the pressure is relatively high owing to the low velocity. As water travelled down the bottom profile, the pressure decreased with increasing velocity. Towards the end of the profile, the pressure head decreases, reaching its minimum just before the water discharges.

At spillway chutes, the understanding of both positive and negative pressures is crucial from design and safety considerations. A balanced positive pressure ensures efficient water discharge. Conversely, negative pressures lead to cavitation. In the current study, the pressure head remained positive along the solid bottom profile, except at the last observation point as shown in Figure 7.

The velocity distribution along the solid bottom profile of the orifice exhibits a significant range, from 23 to 45 m/s. This variation is directly linked to changes in the head, spanning from 40 to 80 m, with the orifice gate opening maintained at 16 m. Figure 8 visually depicts this velocity fluctuation, providing a crucial understanding of how water velocity evolves along the bottom profile under different hydraulic head conditions. Engineers may utilize such data to adopt safety measures and ensure hydraulic efficiency of orifice spillways. High flow velocities exceeding 35 m/s near the discharging end of a chute induce negative pressures (shown in Figure 8), potentially causing cavitation. This risk is heightened when the cavitation index falls below the critical value of 0.2. To pre-empt cavitation-related issues, installing an offset type aerator becomes imperative, acting as a preventive measure to mitigate the adverse effects of high flow velocities. Design guidelines for aerators are developed mainly via systematic laboratory experiments on large-scale models (Pfister & Hager 2010a, 2010b; Pfister 2011). The geometry of an aerator for orifice spillways consists of an offset, aeration ramp and air vent. Offsets and aeration ramps separate the flow from spillway surface and form a cavity for the induction of air at the lower nappe, while the air vent supplies air to the cavity (Anton *et al*. 2023). A flatter bottom profile helps to prevent high flow velocities and resultant negative pressures along the solid bottom profile. Utilizing a value of k greater than 4, such as 4.2 or 4.3, in the trajectory profile equation ($X^2 = 4yh_c$) contributes to achieving a comparatively smoother profile.

4. CONCLUSIONS

A physical model study was conducted to hydraulically investigate the flows through sharp-edged large orifices. The model was built at a 1:100 scale by considering discharge and space constraints. It was operated at various gate openings (10–16 m, in 2 m increments) and water heads (40–80 m, in 10 m increments). Upper and lower nappe profiles of a water jet and discharge coefficients were observed. A solid bottom profile (chute) was designed considering the lower nappe profiles. After

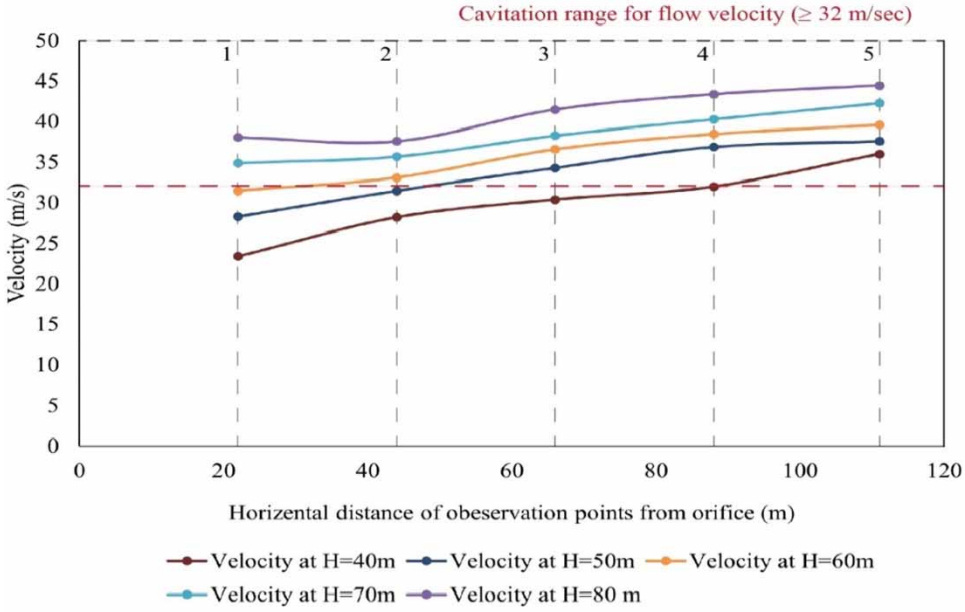

Figure 8 | Velocity variation along the bottom profile at various heads and a 16-m gate opening.

installation of the chute, the upper nappe profiles, discharge coefficients, pressures, and velocities were measured under diverse operational scenarios.

The comparison between upper and lower profiles and the results of the trajectory profile equation revealed good agreement, underscoring the reliability of the model. However, small variations in trajectories signify the sensitivity of the profiles to different factors. Particularly, the C_v, averaging at 0.926, emerged as a critical factor. The variation in the coefficient of velocity significantly impacts the coefficient k of the trajectory profile equation. The maximum k value in this study was 3.63, slightly below the conventional threshold of 4. This deviation implies a steep curvature of the solid bottom profile (chute). Consequently, the curvature of the chute was designed using k value at 4.

The flows on the chute exhibited very high velocities ($v > 35$ m/s) and negative pressures near the discharging end, particularly at heads exceeding 40 m. This suggests that a k value exceeding 4 could yield a more suitable curvature for the 16 m orifice opening at heads above 40 m. In the absence of achieving $k > 4$, there's a recommendation to install an offset type of aerator to prevent cavitation damages, emphasizing the critical role of trajectory profile parameters in ensuring optimal performance of orifice spillways.

Upper nappe profiles clearly deviated from the USBR profiles at all models' operational scenarios before installation of the solid bottom profiles. The installation of solid bottom profiles significantly improved the alignment between upper nappe profiles and USBR profiles. This improvement in alignment highlights the importance of a solid bottom profile in determining upper nappe profiles. Despite the alignment, discrepancies persist, as the USBR equation lacks consideration for head variation. The solid bottom profile also contributed to enhancing the discharge coefficient, with a notable improvement from 0.66 to 0.74 at an 80-m head. These findings are crucial for refining roof profiles and optimizing discharge coefficients in orifice spillway design. Therefore, it is required to investigate the upper nappe profile for different combinations of heads and orifice openings to standardize the roof profile of orifice spillways.

DATA AVAILABILITY STATEMENT

All relevant data are included in the paper or its Supplementary Information.

CONFLICT OF INTEREST

The authors declare there is no conflict.

REFERENCES

Adam, N. J., De Cesare, G., Schleiss, A. J., Richard, S. & Muench-Alligné, C. 2016 Head loss coefficient through sharp-edged orifices. *IOP Conference Series: Earth and Environmental Science* **49** (6), 062009. https://doi.org/10.1088/1755-1315/49/6/062009.

Adam, N., De Cesare, G. & Schleiss, A. 2019 Influence of geometrical parameters of chamfered or rounded orifices on head losses. *Journal of Hydraulic Research* **57** (2), 263–271. doi:10.1080/00221686.2018.1454518.

Amirkhani, M., Bozorg-Haddad, O., Azarnivand, A. & Loáiciga, H. A. 2017 Multiobjective optimal operation of gated spillways. *Journal of Irrigation and Drainage Engineering* **143** (2). https://doi.org/10.1061/(ASCE)IR.1943-4774.0001132.

Anton, J., Sebastien, E. & Jorge, M. 2023 Advances in spillway hydraulics: From theory to practice. *Water* **15**, 2161. https:// doi.org/10.3390/w15122161.

Babu, K. J. M., Gowda, C. J. G. & Ranjith, K. 2018 Numerical study on performance characteristics of multihole orifice plate. *IOP Conference Series: Materials Science and Engineering* **376** (2018), 012032. doi:10.1088/1757-899X/376/1/012032.

Bansal, R. K. 2010 *A Textbook of Fluid Mechanics and Hydraulic Machines*, 9th edn.. Laxmi Publications, New Delhi, p. 1102. ISBN:978-81-318-0815-4.

Bhattarai, R. & Sharma, N. R. 2017 Effect of orifice size on spillway discharge capacity of embankment dams. *Journal of Hydraulic Engineering* **143** (4), 04017090.

Bhosekar, V. V., Patnaik, S. R., Gadge, P. P. & Gupta, I. D. 2014 Discharge characteristics of orifice spillway. *Int. J. Dam Eng.* **XXIV** (1), 5–18.

Bos, M. G. 1989 *Discharge Measurement Structures*. International Institute for Land Reclamation and Improvement, The Netherlands.

Chanson, H. 1999 *The Hydraulics of Open Channel Flow*. Arnold, London.

Daneshfaraz, R., Norouzi, R., Ebadzadeh, P., Francesco, S. D. & Abraham, J. P. 2023 Experimental study of geometric shape and size of sill effects on the hydraulic performance of sluice gates. *Water* **15** (2), 314. https://doi.org/10.3390/w15020314.

Essien, S., Archibong-Esoa, A. & Laoa, L. 2019 Discharge coefficient of high viscosity liquids through nozzles. *Experimental Thermal and Fluid Science* **103** (2019), 1–8. https://doi.org/10.1016/j.expthermflusci.2019.01.004.

Gadge, P. P., Jothiprakash, V. & Bhosekar, V. V. 2016 Physical and numerical model studies for lower and upper nappe profiles of sharpedged large orifice. *ISH Journal of Hydraulic Engineering* **22** (3), 227–235. https://doi.org/10.1080/09715010.2016.1165635.

Gadge, P. P., Jothiprakash, V. & Bhosekar, V. V. 2019 Hydraulic design considerations for orifice spillways. *ISH Journal of Hydraulic Engineering* **25** (1), 12–18. https://doi.org/10.1080/09715010.2018.1423579.

Haghbin, M. & Sharafati, A. 2022 A review of studies on estimating the discharge coefficient of flow control structures based on the soft computing models. *Flow Measurement and Instrumentation* **83**. doi: 10.1016/j.flowmeasinst.2021.102119.

Hussain, S., Hussainn, A. & Ahmad, Z. 2014 Discharge characteristics of orifice spillway under oblique approach flow. *Flow Measurement and Instrumentation* **39** (2014), 9–18. http://dx.doi.org/10.1016/j.flowmeasinst.2014.05.022.

Hussain, A., Ahmad, Z. & Ojha, C. S. P. 2016 Flow through lateral circular orifice under free and submerged flow conditions. *Flow Measurement and Instrumentation* **52**, 57–66. https://doi.org/10.1016/j.flowmeasinst.2016.09.007.

Jithish, K. & Ajay Kumar, P. 2015 Analysis of turbulent flow through an orifice meter using experimental and computational fluid dynamics simulation approach – A case study. *International Journal of Mechanical Engineering Education* **43** (4), 233–246. https://doi.org/10.1177/0306419015604432.

Jothiprakash, V., Bhosekar, V. V. & Deolalikar, P. B. 2015 Flow characteristics of orifice spillway aerator: Numerical model studies. *ISH Journal of Hydraulic Engineering* **21** (2), 216–230. https://doi.org/10.1080/09715010.2015.1007093.

Khatsuria, R. M. 2013 *Hydraulics of Spillway and Energy Dissipaters*. Marcel Dekker publication, New York.

Lienhard, J. H. 1984 Velocity coefficients for free jets from sharp-edged orifices. *Journal of Fluid Engineering* **106**, 12–17.

Maher, H. A., Alomar, O. R. & Mohamed, I. A. 2019 Effects of varying orifice diameter and Reynolds number on discharge coefficient and wall pressure. *Flow Measurement and Instrumentation* **65** (2019), 219–226. https://doi.org/10.1016/j.flowmeasinst.2019.01.004.

Mahmoudi-Rad, M. & Najafzadeh, M. 2022 Role of dissipation chamber in energy loss of vortex structures: Experimental evaluation. *Flow Measurement and Instrumentation* **88**. https://doi.org/10.1016/j.flowmeasinst.2022.102232.

Mahmoudi-Rad, M. & Najafzadeh, M. 2023 Experimental evaluation of the energy dissipation efficiency of the vortex flow section of drop shafts. *Scientific Reports* **13**, 1679. https://doi.org/10.1038/s41598-023-28762-2.

Mahtabi, G. & Arvanaghi, H. 2018 Experimental and numerical analysis of flow over a rectangular full-width sharp-crested weir. *Water Science and Engineering* **11** (1), 75–80. https://doi.org/10.1016/j.wse.2018.03.004.

Mali, C. R., Patwardhan, A. W., Pandey, G. K., Banerjee, I. & Vinod, V. 2020 CFD study on the effect of various geometrical parameters of honeycomb type orifices on pressure drop and cavitation characteristics. *Nuclear Engineering and Design* **370** (2020), 110880. https://doi.org/10.1016/j.nucengdes.2020.110880.

Manzano-Miura, N., Gloutak, D. & Bewley, G. P. 2022 Characterization of a turbulent flow with independent variation of mach and reynolds numbers. *Experiments in Fluids* **63** (2), 44. https://doi.org/10.1007/s00348-022-03390-0.

Mozaffari, S., Amini, E., Mehdipour, H. & Neshat, M. 2022 Flow discharge prediction study using a CFD-Based numerical model and gene expression programming. *Water* **14**, 650. https://doi.org/10.3390/w14040650.

Nguyen, C. & Wang, L. 2015 Physical and numerical model of flow through the spillways with a breast wall. *KSCE Journal of Civil Engineering* **19** (7), 2317–2324.

Pfister, M. 2011 Chute aerators: Steep deflectors and cavity sub pressure. *Journal of Hydraulic Engineering* **137** (10), 1208–1215.

Pfister, M. & Chanson, H. 2014 Two-phase air-water flows: Scale effects in physical modeling. *Journal of Hydrodynamics*, *Series B* **26** (2), 291–298. http://dx.doi.org/10.1016/S1001-6058(14)60032-9.

Pfister, M. & Hager, W. H. 2010a Chute aerators I: Air transport characteristics. *Journal of Hydraulic Engineering* **136**, 352–359.

Pfister, M. & Hager, W. H. 2010b Chute aerators. II: Hydraulic design. *Journal of Hydraulic Engineering* **136**, 360–367.

Pfister, M. & Hager, W. H. 2014 History and significance of the Morton number in hydraulic engineering. *Journal of Hydraulic Engineering* **140** (5), 291–298. https://doi.org/10.1061/(ASCE)HY.1943-7900.0000870.

Prajakta, P., Gadge, V., Jothiprakash, V. & Bhosekar, V. V. 2016 Physical and numerical model studies for lower and upper nappe profiles of sharp-edged large orifice. *ISH Journal of Hydraulic Engineering*. https://doi.org/10.1080/09715010.2016.1165635.

Pu, J. H., Hussain, K., Shao, S. D. & Huang, Y. F. 2014 Shallow sediment transport flow computation using time-varying sediment adaptation length. *International Journal of Sediment Research* **29** (2), 171–183. https://doi:10.1016/S1001-6279 (14)60033-0.

Pu, J. H., Huang, Y., Shao, S. & Hussain, K. 2016 Three-gorge dam fine sediment pollutant transport: Turbulence SPH model simulation of multi-fluid flows. *Journal of Applied Fluid Mechanics* **9** (1), 1–10. doi:10.18869/acadpub.jafm.68.224.23919.

Pu, J. H., Wei, J. & Huang, Y. F. 2017 Velocity distribution and 3D turbulence characteristic analysis for flow over water-worked rough bed. *Water* **9** (9), 668. doi: 10.3390/w9090668.

Rezazadeh, S., Manafpour, M. & Ebrahimnejadian, H. 2020 Three-dimensional simulation of flow over sharp-crested weirs using volume of fluid method. *Journal of Applied Engineering Sciences* **10** (1), 75–82. doi:10.2478/jaes-2020-0012.

Sarwar, M. K., Chaudary, Z. A., Bhatti, M. T. & Khan, D. 2016 Evaluation of Air vents and ramp angles on the performance of orifice spillway aerators. *Journal of Engineering and Applied Sciences* **35** (1), 85–93. doi:10.25211/jeas.v35i1.277.

Swamee, P. K., Ojha, C. S. P. & Kumar, S. 1998 Discharge equation for rectangular slots. *Journal of Hydraulic Engineering* **124** (9), 973–974. https://doi.org/10.1061/(ASCE)0733-9429(1998)124:9(973).

USBR 1980 *Hydraulic Laboratory Techniques*, *A Water Resources Technical Publication*. U.S, Bureau of Reclamation Denver, Colorado.

USBR 1987 *Design of Small Dams*. United States Bureau of Reclamation 3rd edition, US Govt. printing office, Washington, DC.

Vatankhah, A. R. & Rafeifar, F. 2020 Analytical and experimental study of flow through elliptical side orifices. *Flow Measurement and Instrumentation* **72** (2020), 101712. https://doi.org/10.1016/j.flowmeasinst.2020.101712.

Wang, W., Cao, X., Kong, X. & Wu, Y. 2020 An experimental study on the discharge coefficient of a sharped-edged hydraulic orifice. *Journal of Physics: Conference Series* **1605** (2020), 012087. doi:10.1088/1742-6596/1605/1/012087.

First received 21 January 2024; accepted in revised form 16 February 2024. Available online 28 February 2024